PARALLEL PROCESSING TECHNIQUE FOR ACOUSTIC TOMOGRAGHY OF MULTILAYERS

R. B. Mignogna, R. S. Schechter and H. H. Chaskelis
Naval Research Laboratory
Washington, DC 20375-5000

P. P. Delsanto and L. Ferrero
Politecnico di Torino
10129 Torino, Italy

R. Kline and C. Sullivan
University of Oklahoma
Norman, OK 73019

INTRODUCTION

Computerized tomography (CT) is one of the most efficient tools for the nondestructive inspection of a material specimen. Depending on the nature of the application (e.g. in medicine, mechanics or geophysics) and of the particular requirements of the situation, different types of radiation (waves) may be used, thus giving different information about the material properties. For example in diagnostic medicine, x-ray transmission CT gives an attenuation map, which allows different tissues to be distinguished. In the case of x-rays, this type of wave passes through an entire material structure in an almost straight line.

In the characterization of structural materials, however, both the ultrasonic propagation velocity and signal amplitude are relevant quantities. Therefore acoustic tomography, based on time-of-flight and attenuation for different acoustic paths, may be preferable or even necessary. However, the bending of rays in nonhomogeneous media and the directional dependence of the propagation velocity and direction in nonhomogeneous anisotropic materials have so far presented insurmountable difficulties for a general treatment. We propose a method to overcome these difficulties, based on the use of the Connection Machine (CM).

The CM is a massively parallel computer with a large number of processors (many thousand or even millions, if virtual processors are also included), connected in a programmable way, in the framework of a fixed physical wiring scheme. The availability of such a large number of processors, all working simultaneously and independently on the solution of the same problem, has the obvious advantage of decreasing the computer time by a factor of approximately the number of CM processors [1]. It also allows an opportunity to efficiently reformulate the problem to be studied

Review of Progress in Quantitative Nondestructive Evaluation, Vol. 12
Edited by D.O. Thompson and D.E. Chimenti, Plenum Press, New York, 1993

and modify the approach to suit the special requirements and capabilities of the CM.

In our approach, the material is divided into a grid of "cells" in a one-to-one correspondence with the CM processors. The rules governing the wave propagation from cell to cell are input to each processor by means of an iteration equation. The coefficients of the iteration equation depend on the physical properties of the cell and are input as initial data or addressed at any time during computation. Since all of the processors are independent, each cell may have different physical properties, so that almost any arbitrarily complex medium can be treated. The efficiency of our approach and its speed, due to the tremendous computer time savings provided by the parallel processing capability of the CM, have already been demonstrated in several preliminary applications [2-5] of the forward problem of wave propagation. We also take advantage of the parallel processing to drastically speed up the algebraic reconstruction technique (ART), with proper modifications to the formalism.

The entire process is iterative, consisting of a forward part and an inversion routine. The forward part models how the wave propagates through the structure based, initially, on 'guessed' values of the physical properties. The inversion routine compares the results obtained from the forward model with actual data. The difference between the real data and the forward calculation is used by the inversion routine to adjust the 'guessed' physical properties for the forward model. This process is then repeated, continuously adjusting the physical properties, until convergence is reached. As a first step toward the goal of general acoustic tomography, we present our results for acoustic tomography of multilayers.

THE ITERATION EQUATIONS

Let us assume, for simplicity, that we want to study the wave propagation in a homogeneous isotropic material. We also assume that there is complete symmetry, both in the material and in the source pulse, with respect to one of the coordinates (say z). Thus the problem becomes effectively two-dimensional and the acoustic wave equation

$$\partial(S_{klmn} w_{m,n})_l = \rho \ddot{w}_k \tag{1}$$

can be written as

$$\begin{aligned} \rho\ddot{u} &= (\lambda+2\mu)\frac{\partial^2 u}{\partial x^2} + \mu\frac{\partial^2 u}{\partial y^2} + (\lambda+\mu)\frac{\partial^2 v}{\partial x \partial y} \\ \rho\ddot{v} &= (\lambda+2\mu)\frac{\partial^2 v}{\partial y^2} + \mu\frac{\partial^2 v}{\partial x^2} + (\lambda+\mu)\frac{\partial^2 u}{\partial x \partial y} \end{aligned} \tag{2}$$

In Eqs. (1) and (2) S_{klmn} is the stiffness tensor, w the displacement vector, ρ the density, λ and μ are the Lame' constants and u and v are the x and y components of w, respectively. The iteration equations for the single homogenous isotropic material have been presented else where[3]. We now consider a two layered material, the first layer having an acoustic impedance, Z, and material properties, ρ, λ and μ. The second layer having acoustic impedance, Z', and material properties, ρ', λ' and μ' as shown in Fig. 1. At the horizontal boundary passing through point P, we require the continuity of both displacements (u=u', v=v') and stresses ($\tau_{11}=\tau_{11}'$, $\tau_{12}=\tau_{12}'$) along the boundary (interface).

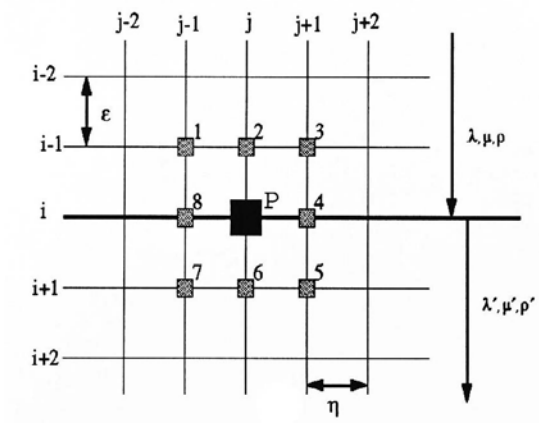

Fig. 1. Processors utilized for iteration equation at time t+1 at the point P. The interface shown here, passes through point P, along i.

Transforming and simultaneously solving the equations of motion and the boundary conditions into finite difference equations (FDE) yield

$$u_{i,j,t+1} = \tilde{\alpha}u_2 + \tilde{\alpha}'u_6 + \tilde{\beta}(u_4+u_6) + \tilde{\gamma}(v_1-v_3) - \tilde{\gamma}'(v_5-v_7) + \tilde{\chi}(v_4-v_8) - 2\tilde{\xi}u - u_{t-1}$$
$$v_{i,j,t+1} = \tilde{\alpha}v_2 + \tilde{\alpha}'v_6 + \tilde{\beta}(v_4+v_6) + \tilde{\gamma}(u_1-u_3) - \tilde{\gamma}'(u_5-u_7) - \tilde{\chi}(v_4-v_8) - 2\tilde{\xi}u - u_{t-1} \qquad (3)$$

where $\alpha = \underline{\beta} = (\frac{v_L}{v})^2$, $\underline{\alpha} = \beta = (\frac{v_T}{v})^2$, $\gamma = \frac{(v_L^2 - v_T^2)}{4v^2}$, $\chi = \psi'\gamma' - \psi\gamma$, $\psi = \frac{(\lambda-\mu)}{(\lambda+\mu)}$,

$\xi = \alpha+\beta-1$, $v_L = \sqrt{\frac{(\lambda+2\mu)}{\rho}}$, $v_T = \sqrt{\frac{\mu}{\rho}}$, $Z = \rho v$, $Z' = \rho' v$, $Z_L = \rho v_L$, $Z_T = \rho v_T$,

$\tilde{\alpha} = T\alpha$, $\tilde{\alpha}' = T\alpha'$, $\tilde{\beta} = \frac{(T\beta + T'\beta')}{2}$, $\tilde{\gamma} = T\gamma$, $\tilde{\gamma}' = T'\gamma'$, $\tilde{\xi} = \frac{(T\xi + T'\xi')}{2}$, $T = \frac{2Z}{(Z+Z')}$,

$T' = \frac{2Z'}{(Z+Z')}$, $\underline{\tilde{\alpha}} = T\underline{\alpha}$, $\underline{\tilde{\alpha}}' = T\underline{\alpha}'$, and $\underline{\tilde{\beta}} = \frac{(T\underline{\beta} + T'\underline{\beta}')}{2}$. The numbered subscripts on u and v in Eq. 3 imply the following: 1 -> (i-1,j-1,t), 2 -> (i-1,j,t), 3 -> (i-1,j+1,t), 4 -> (i,j+1,t), etc., as shown in Fig. 1. The components, u and v, with subscripts t-1 or without any subscript imply: t-1 -> (i,j,t-1) and no subscript implies (i,j,t). The iteration equation is, therefore, a function of one step in the past and the present values, including the 8 nearest neighbors. This formulation holds for any number of layers.

The cell velocity that was used for the CM program was $v = \sqrt{2}v_L(\text{maximum})$, $v_L(\text{maximum})$ being the maximum longitudinal velocity of all the layers or the largest expected velocity of any material in the layers. This cell velocity criteria is in agreement with von Neumann criterion[6]

$$v \geq \sqrt{v_L^2 + v_T^2}. \qquad (4)$$

From this and the time increment δ the cell spacing is determined, $\varepsilon = \eta = v\delta$. In addition, the number of nodes per smallest wavelength was 16.

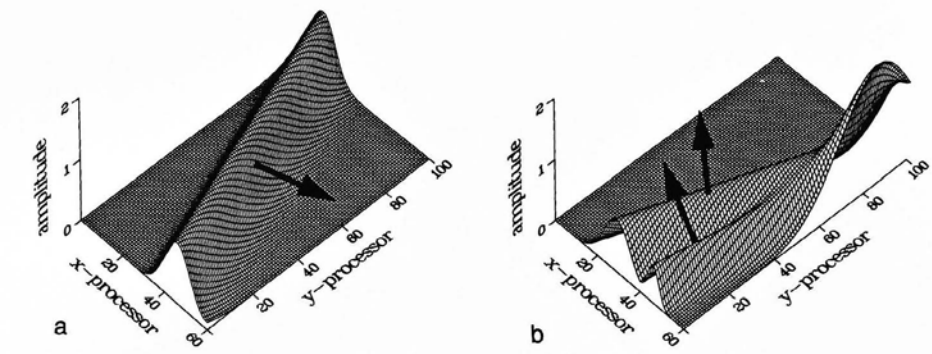

Fig. 2. A longitudinal wave, gaussian in time and infinite in extent, propagated at 20 degrees with respect to the normal of the free boundary. a) Shows the wave approaching the boundary, b) shows the reflected longitudinal and shear waves.

EXAMPLE OF THE FORWARD CALCULATION

Various test cases were run to ensure that the forward calculations were working properly, such as various layers of materials, spatially finite and infinite source waves, oblique incidence above and below the first critical angle, etc. An Epstein layer was also modelled as a material in which a continuous change in impedance occurred with respect to one direction. The Epstein layer was broken up into 50 layers (since the CM model is discrete) and has an impedance change of a factor of 2, that is, the impedance of the last layer is twice the impedance of the first layer. A finite incident pulse, 5 wavelengths long and gaussian in time, was generated at an oblique angle to the direction of material change. Continuous refraction is predicted for this case and was observed when the model was run. These forward cases were displayed on the CM frame buffer. The frame buffer is a parallel graphics display on the CM that permitted the various cases that we examined to be viewed as a video movie. As an example, the frame rate was of the order of 100 milliseconds per frame for a 256 by 512 2-dimensional processor array. The frame buffer accounted for most of the 100 milliseconds per frame. The forward calculation runs at about 3 Gflops per second. A simple case of mode conversion at a free boundary is shown in Fig. 2. A longitudinal wave, gaussian in time and infinite in extent was propagated at 20 degrees with respect to the normal of the free boundary. Figure 2a shows the wave approaching the boundary, Fig. 2b shows the reflected longitudinal and shear waves.

INVERSION

The inversion routine we are developing is based on the algebraic reconstruction technique (ART). Consider a rectangular sample of dimensions h by a, divided into a grid of I rows by J columns, shown in Fig. 3. Also consider M transmitters T_m (m=1,M) and N receivers R_n (n=1,N) located anywhere on the boundaries of the grid. Along an initially straight path p=(m,n), from T_m to R_n, the path crosses Q_p cells. The distance traveled through cell q at (i,j) is l_{pq}. The time needed to cross cell q is

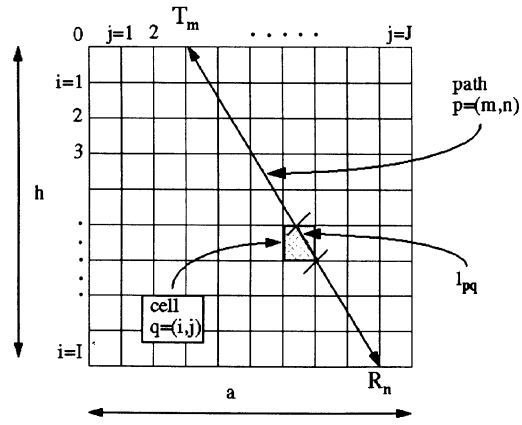

Fig. 3. Grid for reconstructing tomogram. Path p goes from T_m to R_n, passes through cell q=(i,j). Distance of path p in cell q is l_{pq}.

$t_{pq}=l_{pq}S_{ij}$, where S_{ij} is the slowness in cell q. The total time of flight from Tm to Rn along path p is:

$$t_p = \sum_{q=1}^{Q_p} t_{pq} = \sum_{i=1}^{I}\sum_{j=1}^{J} l_{p(q=(i,j))} S_{ij} \qquad (5)$$

where $l_{pq}=0$ for all cells not crossed by path p. Let the corresponding experimental (or simulated) time of flight between T_m and R_n be $\tilde{t}_p$ and the actual slowness values for each cell $\tilde{S}_{ij}$ (which is our aim to determine). A change in the time of flight can be expressed as a change in the slowness of the cell as

$$\Delta t_p = \sum_q l_{pq}\Delta S_q \qquad (6)$$

where $\Delta t_p = \tilde{t}_p - t_p$, $\Delta S_q \equiv \Delta S_{ij} = \tilde{S}_q - S_q$ and $S_q=S_{ij}$. If the change in slowness of a cell is made proportional to the distance traveled in the cell we can write

$$\Delta S_q = l_{pq}c \qquad (7)$$

from Eqs. 5 and 6 it follows that

$$c = \frac{\Delta t_p}{\sum l_{pq}^2}. \qquad (8)$$

Therefore, for each path, the corrections to the slowness for each cell are

$$\Delta S_q = \frac{\Delta t_p l_{pq}}{\sum l_{pq}^2} \tag{9}$$

RESULTS

Figure 4a and 4b show a simulated, three-layered material and the reconstructed tomogram, respectively. The sample was divided into a 15 by 15 grid, with five processors per layer (normal to the layer). A total of 1800 ray paths were used. The transmitters (simulated) were located at every grid point on the top and bottom of the three-layered material and the receivers were positioned at all of the grid points at the surface of all four sides. The entire calculations took less that 2 minutes. This test case used a rather small number of ray paths for the inversion. The more ray paths used, the more efficient parallel processing becomes. The reconstructed tomogram best matches the simulated layered material in the center of the grid, as expected since the density of ray paths is higher. As can be seen in Fig. 4b, the match is not as good at the corner or along the edges of the grid because this where the ray path density is low.

DISCUSSION

ART is a serial method, based on serial calculations. The CM permits the entire problem to be parallelized. We are modifying ART in pieces, converting sequential methods to parallel methods. Figure 5 presents a general flow chart of our current program, indicating what sections of the

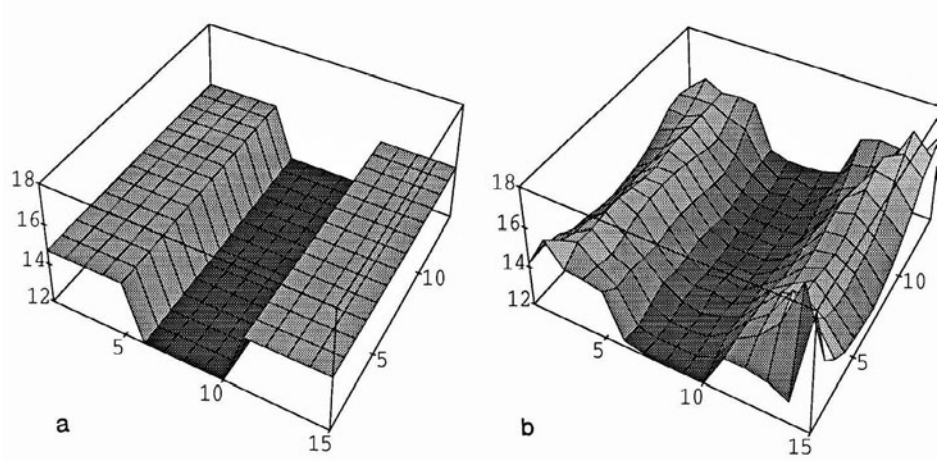

Fig. 4. a) Simulated, three-layer material. b) Reconstructed tomogram of the three-layer material. Vertical units are arbitrary.

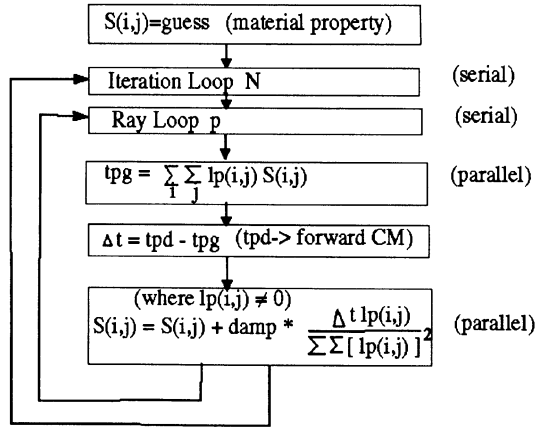

Fig. 5. Flow chart of the modified ART type routine being used. Areas that are parallel and those that are still serial are indicated.

program are parallel and which are still serial. The current evaluation tests that we are running use a rather small number of paths (transmitter-receiver pairs) to ease trouble shooting of the program. Once the method is in place, extension to large grids and more general cases is straight forward and the utility of parallel programing for acoustic tomography will become self evident.

ACKNOWLEDGEMENT

The research reported here was done under sponsorship of the Office of Naval Technology.

REFERENCES

1. P. J. Denning and W. F. Tichy, Science, 1222 (1990).
2. P. P. Delsanto, T. Whitcombe, H. H. Chaskelis and R. B. Mignogna, "Connection Machine Simulation of the Ultrasonic Wave Propagation in Materials I: The One-dimensional Case, Wave Motion, 16 (1992) p. 65-80.
3. P. P. Delsanto, T. Whitcombe, H. H. Chaskelis and R. B. Mignogna, in Review of Progress in Quantitative Nondestructive Evaluation Vol 9A, D.O. Thompson and D.E. Chimenti eds.,Plenum Press, New York, (1990) p. 141-8.
4. P. P. Delsanto, T. Whitcombe, N. K. Batra, H. H. Chaskelis and R. B. Mignogna, ibid. Vol. 10 (1991) p. 241-8.
5. P. P. Delsanto, H. H. Chaskelis, R. B. Mignogna, T. V. Whitcombe and R. S. Schechter, ibid. Vol. 11 (1992) p. 113-120.
6. Z. S. Alterman and D. Loewenthal, Geophys. J. R. Astr. Soc., 20 (1970) p. 101-126.